Orelma, Hannes; Kunnari, Vesa; Yamamoto, Akio; Valkonen, Mikko; Rautkari, Lauri; Korpela, Antti

Improving mechanical performance and functionality of birch veneer with mechano-enzymatic microfibrillated cellulose coating

Published in:
Cellulose

DOI:
10.1007/s10570-023-05059-1

Published: 01/03/2023

Document Version
Publisher's PDF, also known as Version of record

Cellulose (2023) 30:3237–3254
https://doi.org/10.1007/s10570-023-05059-1

ORIGINAL RESEARCH

Improving mechanical performance and functionality of birch veneer with mechano-enzymatic microfibrillated cellulose coating

Hannes Orelma · Vesa Kunnari · Akio Yamamoto · Mikko Valkonen · Lauri Rautkari · Antti Korpela

Received: 7 October 2022 / Accepted: 12 January 2023 / Published online: 30 January 2023

Abstract In this study, we investigated the coating of birch veneers (BVs) with mechano-enzymatically manufactured microfibrillated cellulose (meMFC) to improve mechanical strength and functionality. The meMFC has a broad particle size distribution and similar chemistry to lignocellulose materials, which are both beneficial properties in the coating of wood products. The veneer coating trials were carried out with a spray coating system developed to coat controllable thin coating layers. The spray coating produced uniform layers, which smoothened the BV surface significantly and was verified with scanning electron microscope imaging and optical profilometer measurements. The surface energy measurements showed that the meMFC is like cellulose, whereas the BV is like lignin. This observation proposes pre-treatment methods to secure a good adhesion level between the meMFC and BVs. The adhesion and compatibility of meMFC with the BV surface were measured with pull-off tests and surface energy measurements. The adhesion on a native BV surface was limited, while pre-treatment with sanding or using a primer significantly enhanced the adhesion. The meMFC coating slightly improved the BV transverse tensile strength (perpendicular to the wood veneer grain direction). A thermochromic functionality was installed on the BVs using meMFC as a binder. The produced thermochromic BVs displayed thermochromic behaviour; the coating could control the warming of the BVs subjected to solar radiation. The activation of a photocatalytic reaction of a meMFC coating containing TiO_2 was studied on the wood surface under both ultraviolet and fluorescent light, indicating in a reduction of formaldehyde concentrations. The results also showed that wood discolouration was inhibited by meMFC with not only TiO_2 but also only the meMFC coating. This study presents a practical approach to surface-treating wood materials with the meMFC to improve the mechanical and functional properties of wood products.

Keywords Mechano-enzymatic microfibrillated cellulose · Birch veneer · Coating · Adhesion · Compatibility · Thermochromic pigments

H. Orelma (✉) · V. Kunnari · A. Yamamoto · A. Korpela
High-Performance Fibre Products, VTT Technical Research Centre of Finland Ltd, Biologinkuja 7, 02044 Espoo, Finland
e-mail: hannes.orelma@vtt.fi

M. Valkonen · L. Rautkari
School of Chemical Engineering, Department of Bioproducts and Biosystems, Wood Material Science and Technology, Aalto University, Vuorimiehentie 1, 02150 Espoo, Finland

Introduction

Wood materials have already been used for thousands of years to produce dwellings, paper, and other consumer goods (Ennos 2020). Wood-based materials have many unique inherent properties as they are

simultaneously of biobased origin, biodegradable, and recyclable. In recent years, the progressing climate change has caused an immediate need to replace fossil-based materials with lignocellulosics to reduce carbon emissions (Bergman et al. 2014; Sathre and Gustavsson 2009). In general, wood is composed of chemical components that are rapidly biodegradable without forming microplastic-type long-lasting residues (Higuchi 1985). The excellent enzymatic degradability of lignocellulose (LC) is based on the accessible hydroxyl groups of cellulose and hemicelluloses. However, these functional polar substituents simultaneously cause wood to swell in water, causing dimensional instability (Kocaefe et al. 2015).

Additionally, the visual appearance of wood products, such as their smoothness, colour, and light scattering, may need to be improved. Thus, wood materials are always post- or pre-treated to ensure their use in the end applications (Ramage et al. 2017). Unfortunately, many of the current treatment formulations are based on synthetic compounds. Therefore, there is a need to develop more environmentally-friendly protection methods to enhance the inherent properties of wood materials.

Currently, three major treatment strategies for wood have been used: (a) chemical substitution of the hydroxyls of LC; (b) impregnating the wood with preservatives that can eliminate microorganisms or with fire retardants that lower the likelihood of incineration; (c) blocking the surface of the wood to prevent moisture, microorganisms, fire, or light penetrating the cellular structure of the material (Ramage et al. 2017). Painting is the easiest route to protect wood since it can also be applied on a construction site by the end user. A typical paint consists of pigments, binder polymers, extenders, solvents, and additives. The paint composition is always application- and substrate-dependent. Most commercial paints use binders that are synthetic acrylic, alkyd, and epoxy polymers (Stoye et al. 2000). Wood-based materials have already been used in paints as cellulose derivatives for binders and particle fillers for improving paint structure and coverage (Bulian and Graystone 2009; Croll et al. 1986). The role of fillers in paints is crucial since the paint polymers cannot fill the surface roughness (SR) induced pores of the painted surface. Therefore, it is conceivable that an alternative compound between a polymer and microsized filler could be helpful in painting applications of wood to adhere and smoothen the wood surface simultaneously. One potential option for this could be LC-based nanocellulose (NC).

Nanocellulose is a general name for nanoscale materials covering cellulose nanocrystals, cellulose nanofibrils (CNFs), and bacterial cellulose (Moon et al. 2011). Cellulose nanomaterials have a strong tendency to form hydrogen-bonded networks when water is evacuated from the material during drying (Österberg et al. 2013). Thus, a NC film is a good oxygen barrier that concurrently hinders water transportation through the film to some degree (Hubbe et al. 2017; Lavoine et al. 2012). Nanocellulose materials have also been shown to tightly bind almost any particles, which is useful when using the NCs as binders for other particles (Mattos et al. 2020). The surface hydroxyl groups enable the surface modification of the NC with varying chemistries (Klemm et al. 1998). Control of the surface charge is one widely-used chemical tool. The control can be achieved by using carboxymethylation (Siró et al. 2011) and 2,2,6,6-tetramethyl-piperidine-1-oxyl-mediated oxidation (Saito et al. 2006). An installed anionic charge enhances the fibrillation of wood fibres into NC and increases the film-forming ability of the NC. The cationisation of NC has been shown to make it antimicrobial (Uddin et al. 2017) and to enhance the retention of minerals in cellulose fibres in paper-making applications (Liu et al. 2019). The mechano-enzymatic method is one environmentally-friendly approach to producing coarse NC (Pere et al. 2020). This mechano-enzymatic microfibrillated cellulose (meMFC) has a polydisperse size distribution and a tendency to form a paste in high solids content (Pere et al. 2020). Moreover, the given material differs from conventional mechanically made NC because it does not shrink much when water is removed due to its higher solids content (Klar et al. 2019).

Wood construction materials face external stresses during service time, such as humidity and temperature changes caused by fluctuations in solar radiation. Darkly-tinted exterior surfaces absorb more solar radiation, which causes rapid temperature and humidity changes in wood materials, leading to cracking (Taha et al. 1992). However, white exterior surfaces absorb less solar radiation, leading to fewer surface temperature changes and a reduced need for cooling down the buildings. Then again, the white surfaces may expose the materials to microbial action in wet

conditions. For example, it is reported that black and white exterior wood panels may reach surface temperatures of 80 and 35 °C under direct sunlight (Ahonen 1995). In the literature, an idea has been presented to make houses reactive to temperature changes by using thermoactivated coatings that change in colour as a function of external temperature. The thermoactive response would be based on chemical compounds with thermochromism behaviour (Abdellaoui et al. 2020). These coatings can control the microclimate of buildings by controlling the energy-absorbing or -reflecting behaviour of building surfaces (Karlessi et al. 2009; Zheng et al. 2015). These studies reported that it is possible to achieve significant energy savings in warm areas or regions with a cold winter and warm summer with thermoactive coatings compared to thermally inactive ones.

In addition, little is known about the potential of meMFC on wood surfaces as a coating material. Few studies have attempted to define the potential of CNFs as a coating material to add functionality to the wood surface (Yuan et al. 2021). Since a high affinity exists between the CNFs and wood surface, a certain degree of adhesion occurs due to the strong hydrogen bonds at the interface when the CNFs are applied to a wood surface (Cheng et al. 2016; Yano et al. 2018). The main advantage of the CNFs is their high specific surface area (Yano et al. 2018), which provides efficient functionality. Titanium dioxide (TiO_2) is a photocatalyst that could decompose contaminants, including volatile organic compounds (VOCs), when exposed to light irradiation at a specific wavelength range(Ichiura et al. 2003). The effects and mechanism of the photocatalytic (PC) reaction of TiO_2 have been widely studied since the seminal *Nature* publication in 1972 (Fujishima and Honda 1972). The research on wood surface-treatment with TiO_2 has attracted considerable critical attention in recent years, aiming to improve ultraviolet (UV) protection (Pánek et al. 2020; Pori et al. 2016), hydrophobicity and self-cleaning (Pandit et al. 2020; Rao et al. 2016; Xing et al. 2020), and VOC removal (Zhu et al. 2016) and anti-fungal capabilities (Chen et al. 2009).

In this study, the use of meMFC (Pere et al. 2020) was investigated for the surface coating of birch veneers (BVs) (Fig. 1). The study investigated how the used meMFC coats adhered to a BV surface. The coating was carried out using a simple spray-coating setup that enabled reasonable coating weight control. It is conceivable that the prepared meMFC with broad size distribution and a high solids content could help protect the wood surface. In general, the small polymeric materials of the meMFC enhance the adhesion, while the larger particles fill the rough surfaces, and the high solids content prevents drying-based shrinkage that may break the formed film. The chemical and physical properties of the meMFC influencing its adhesion to wood surfaces were investigated. The mechanical strength of the BVs was also studied regarding the effect of the coating. The meMFC was also used as a binding matrix for the thermochromic (TC) pigments. The TC activity of the meMFC was studied in laboratory and exterior conditions to demonstrate the usability of the TC meMFC coating. Additionally, the effects of the meMFC containing TiO_2 were studied, focusing specifically on UV protection and VOC removal. The PC reaction was activated with light in the UV and visible wavelength range. The degree of the VOC removal was measured using formaldehyde (HCHO), a major indoor-air pollutant in modern housing. The reflectance and scattering of UV light in TiO_2-doped meMFC were determined by the degree of discolouration of the wood surface. The results show that the meMFC is a potential coating material for BV products and can potentially be used to install active pigments on the surfaces of other wood products.

Experimental section

Materials

Never-dried birch veneer (BVs) with nominal thicknesses of 0.6, 1.0, and 1.5 mm were obtained from Koskisen Oy. The specimens were stored in a freezer room at ca. − 20 °C prior to thawing just before the coating trials. The cellulose source of the meMFC was bleached softwood kraft pulp obtained from Metsä Fibre (Äänekoski bioproduct mill, Finland). Carbohydrate and lignin compositions of the pulp were: cellulose content 81%, hemicelluloses content 18%, and lignin content < 0.5%. Black TC pigment (Chameleon Slurry Black 31 °C, 5102CPT03102EKGL, Batch A9-031121-1T) from LCR Hallcrest with a colour transition temperature in the warming direction of 25.0–32.5 °C and in the cooling direction 29.0–21.0 °C. Orange TC pigment (ChromaZone®

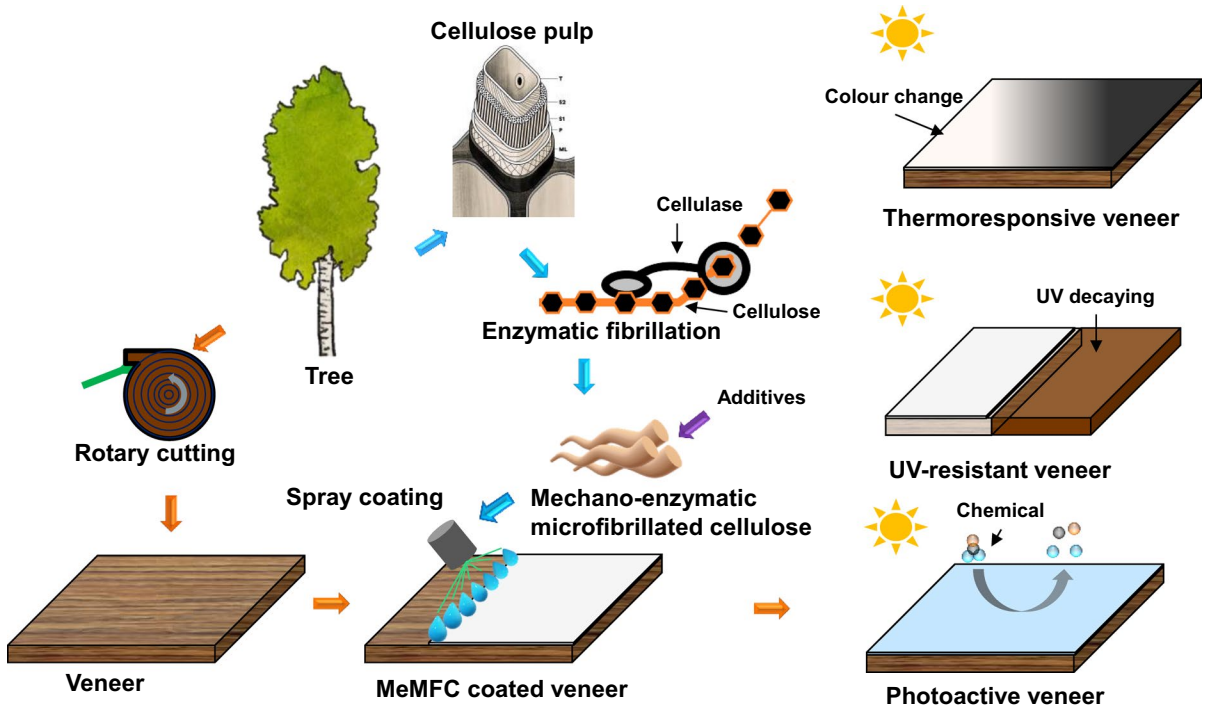

Fig. 1 A schematic illustration of the manufacture of functional meMFC coatings onto rotary cut veneer. Three functional surfaces presented: **a** Thermoresponsive coating with thermochromic pigments, **b** UV-decauing blocking with meMFC, and **c** photodegradation of chemicals with TiO_2

Slurry Orange 31 °C, 5300CPT03106EKG, Batch A9-012320-1) from LCR Hallcrest with colour transition in the warming direction 21.5–33.0 °C and in the cooling direction 29.5–16.0 °C. The TiO_2 used in the study was analytical grade in powder form and purchased from Merck (Darmstadt, Germany). All other chemicals used were laboratory-grade. All water used was purified using a Milli-Q device.

Methods

The preparation of the mechanoenzymatic microfibrillated cellulose (meMFC)

The meMFC used in the study was produced following the procedure reported in (Pere et al. 2020). The process utilises a simultaneous enzymatic action and fibre-to-fibre friction caused by the gentle mixing. The cellulosic pulp was treated at 25 wt.% for 8 h at 70 °C using a two-shaft sigma mixer (Jaygo Incorporated, NJ, USA) running at 25 rpm. The size distribution of the prepared meMFC is shown in Fig. 2. First, the average length-weighted length and width of the pulp fibres were determined using a Metso FiberLab fibre image analyser. Then, the present soluble substances were measured gravimetrically by dialysing the meMFC vs. Milli-Q water in a dialysis tube (Spectra/Por®, molecular weight cut-off 3500 dalton). The produced material was stored in a refrigerator (4 °C) before its use in the coating studies.

Birch veneer coating with the meMFC

With the help of a self-made laboratory spray-coating unit, the meMFC was applied to the BV specimens (Fig. 3). The coating station included a motorised vacuum sledge that fixed the specimens horizontally. The diameter of the spray nozzle and used pressure were ca. 254 µm and 3.5 bar, respectively. The width of the spray was ca. 260 mm. The specimens were placed on the sledge and coated with meMFC at a ca. 10.0 wt.% dry matter content using a constant speed (1 m/min). The coating thickness was adjusted by preparing specimens with multiple coating layers (CLs)

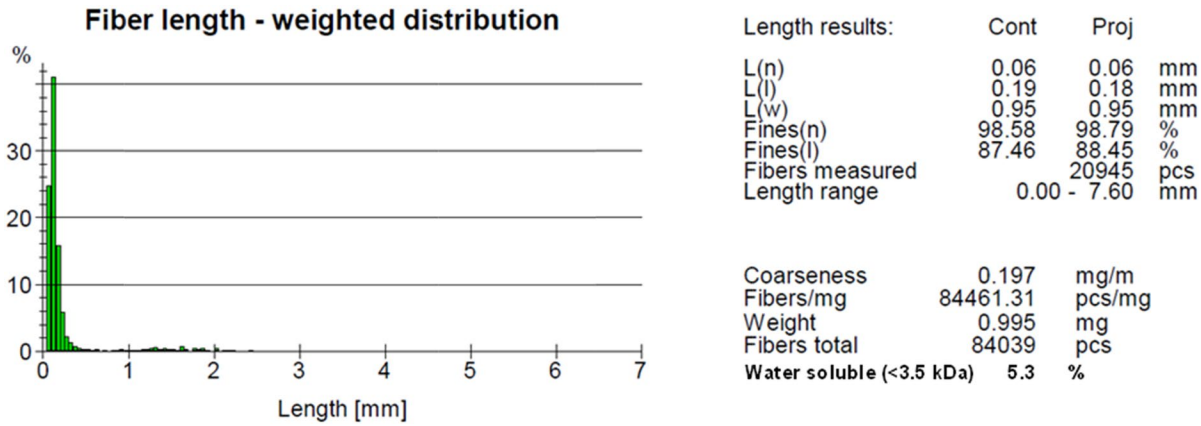

Fig. 2 The fibre length-weighted distribution, average particle sizes, and water-soluble fraction of the prepared meMFC

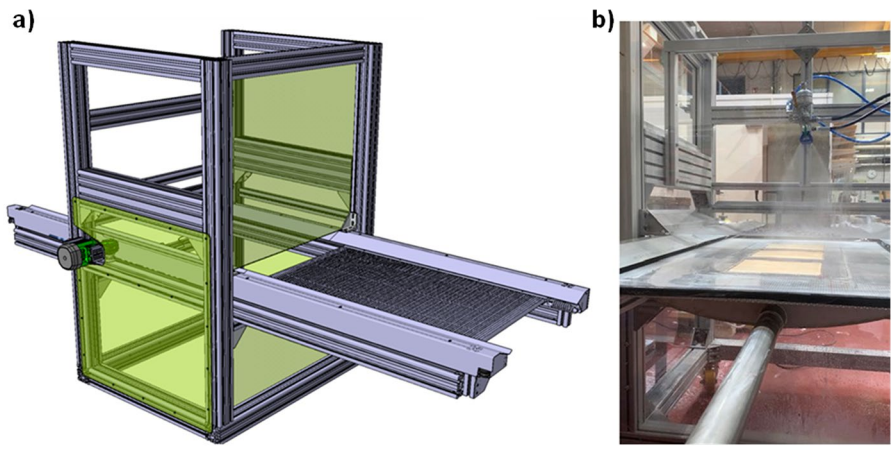

Fig. 3 **a** A schematic illustration of the laboratory-scale coating station. **b** A photograph of spray coating the meMFC coating on the BV specimens

layer-by-layer. The coating amount was measured gravimetrically by balancing the specimen before and after meMFC coating (dry specimens). The coating trials were carried out on dry and wet BV specimens with and without sanding.

The BASF Epotal ECO 3675X primer (a CL coat weight of ca. 2.1 ± 0.5 g/m^2) was also tested to improve the adhesion between the meMFC coating and BVs. The specimen size in the coating studies was kept constant at ca. 15×15 cm^2. The meMFC coating was always applied on the less dense side of the BV specimens. The drying of the coated BVs was carried out with two different methods: (a) hot-air-flow drying (referred to as blower drying, BD) with a blow-air dryer (Harju BG-E3A 3 kW) and (b) in a standard condition (SC) at ca. 20 °C and 65% relative humidity (RH).

Scanning electron microscopy

The scanning electron microscope (SEM) imaging of the coated specimens with an uncoated native BV reference specimen was carried out with a Merlin Field Emission (FE)-SEM (Carl Zeiss NTS GmbH, Germany) with the applied gold sputter coatings (ca. 30 mA, 30 s). The electron gun voltage was constant at ca. 3.0 kV with a grid current of ca. 60 pA. The pixel resolution of the SEM was $2\,048 \times 1\,536$.

Fourier-transform infrared microscopy (FTIR)

FTIR spectroscopy was used to study the MEMFC coated BVs. The characterization was performed using a Thermo Scientific Nicolet iS50 FT-IR spectrometer with an ATR diamond (Thermo Scientific,

USA). All spectra were obtained from 32 scans with a resolution of 4 cm^{-1} and absorption mode using a wavelength range of 400 to 4000 cm^{-1}. The measurements were conducted with uncoated and meMFC coated BVs with a coat weight of 29 g/m^2. At least three repetitions per sample were conducted.

Surface free energy measurements with a water contact angle goniometer

Water contact angle (WCA) measurements were conducted with an Attention Theta Optical Tensiometer (Biolin Scientific, Sweden). The measurements were performed at ca. 23°C and 50% RH with Milli-Q water as the probe liquid with a droplet volume of ca. 4.0 µl, and at least five locations were measured from each specimen for statistical accuracy and repeatability. Uncoated native BV specimens were used as references. The surface free energy (SFE) measurements were carried out with four test liquids: water, ethylene glycol, formamide, and 3,3'-diindolylmethane. The SFEs were calculated based on the Lewis acid-base model.

The determination of the strength, adhesion, and SR properties

The transverse tensile strength (TTS) of the BV specimens was measured using a Zwick 1475 universal material testing machine (ZwickRoell Group, Ulm, Germany) equipped with a MTS control system (MTS Systems Corp., Eden Prairie, MN, USA) and a 1 000 N load cell. The specimens were prepared from coated BV sheets with dimensions of ca. 50×150 mm ($w \times l$, the specimen length direction was perpendicular to the wood grain). Uncoated native BV specimens were used as references. Before the test, the specimens were conditioned at ca. 20 °C and 65% RH for at least 1 wk. The loading direction was along the specimen length with a 2.0 mm/min nominal loading speed. The test was initiated with a crosshead clearance of ca. 50 mm. The standard EN 314-1 (Standardization 2004) was used for calculating the TTS of each specimen. Specifically, the effects of the drying methods were determined by conducting the TTS test on BVs at three different BV thicknesses (0.6, 1.0, and 1.5 mm (note. with 1.5 mm BV only coating with CL 1 was tested)) and for three different CLs (1, 2, and 3). The TTS properties were analysed from the sample matrix of the BV specimens (repetitions, $n = 9$).

The adhesion between the meMFC coating and BVs was investigated using pull-off measurements with a Lloyd LS5 tensile tester equipped with a 100 N sensor (AMETEK Measurement & Calibration Technologies, Largo, FL, USA) in standardised laboratory conditions (ca. 50% RH and 23 °C). Aluminium pull stubs (a diameter of ca. 11 mm) were glued to the BV surfaces with epoxy glue. Then, the stub was pulled off from the surface under the tensile tester in a vertical direction from the specimen. The cut-out diameter of the coating under the stub was used to calculate the adhesion strength. At least five replicates were used, while the uncoated native BV specimens functioned as references. Furthermore, the SR of the BV specimens were measured using a Veeco Wyko NT 9100 optical profilometer (Bruker, USA). At least five spots on each specimen were investigated for statistical accuracy and repeatability. The SR values represent the average values calculated from the repetitions.

A thermoresponsive meMFC coating and solar warming studies

The TC meMFC coatings were prepared by mixing a thermochromic (TC) pigment (black and orange colours were tested) in a ca. 10.0 wt.% meMFC dispersion using a blade mixer. The added pigment contents in the meMFCs were ca. 2.5, 8.0, and 20.0 wt.% to the dry matter content of the meMFC. The coated specimens were prepared by masking a constant area of the BV specimens and adding one CL of the TC meMFC coating per the masked area. Uncoated native BV specimens acted as references. The prepared specimens were dried in room conditions. A colour change test was carried out under a heat blower (Harju BG-E3A 3 kW) by controlling the heating with a power switch. The cycling was carried out by visually following when the specimen changed in colour. The field tests were conducted from 8/11 to 12/2021 at ca. 21 °C. The specimens were placed in direct sunlight, and the surface temperature was monitored continuously with a heat camera (Flir C5, Teledyne Flir systems, USA).

The preparation of the BV specimens coated with the meMFC containingTiO_2

The TiO_2-doped meMFC was prepared by mixing the TiO_2 in a meMFC suspension at a ca. 10.0 wt.% of the solids content. The preparation involved stirring the mixture manually with a spatula for over 3 min in a 200 ml beaker. Next, the suspension was applied gap-free to the specimen surface with a paintbrush. After that, the specimens were dried in a conditioning room (20 °C and 65% RH) for at least 24 h before the experiments. Uncoated native BV specimens functioned as references.

The weathering treatment of the BV specimens

The BV specimens were tested using a Suntest CPS + Xenon Weathering instrument (AMETEK Atlas / AMETEK, Inc.; Mount Prospect; IL; USA) which was used to accelerate the degree of discolouration on the BV surfaces with or without the meMFC and its potential TiO_2 doping due to the high radiation levels of the UV light. The colour coordinates of the BV surfaces were measured with a spectrophotometer (Spectrolino, Gretag-Macbeth AG, Regensdorf, Switzerland). Earlywood was chosen for the measurement to reduce the measurement variation (Yamamoto et al. 2017). The colour differences were calculated as the parameter ΔE_{ab}, commonly used for the colour measurement of the wood surface (Yamamoto et al. 2015).

The evaluation of the VOC removal on the coated BVs with gas chromatography with flame-ionisation detection

In the gas chromatography with flame-ionisation detection (FID) experiment, a headspace technique combined with a gas chromatography analysis was performed to verify the activation of the photocatalyst in the meMFC by the light of different wavelengths following the Shimadzu's application note No. G327 with slight modifications. It is important to note that the FID detector cannot see small concentrations of formaldehyde. In this study the formaldehyde levels measured were high that made them visible in the FID detector. Due to these limitation, the results shown here can be used only qualitatively. The BV specimen was prepared from the coated BVs in ca. 1 × 5 cm dimensions and placed in an 18-mm headspace screw-top vial with a nominal usable volume of 20 ml. Approximately a 1.0 µl volume of 36% HCHO solution in analytical grade (Avantor® / VWR International, LLC; Philadelphia; PA; USA) was added to the inner wall of the vial to prepare the sample. The vial was sealed with a metal screw cap with a septum. During the experiment, the vials were placed under either regular fluorescent lights (480 nm, 730 lx) or a UV light (350 nm, 450 lx). The headspace sample was collected with a syringe and immediately injected into a gas chromatograph (GC)-2010 Plus with a flame ionisation detector (FID)-2010 Plus (Shimadzu Corp., Kyoto, Japan) using hydrogen as the carrier gas (ca. 1.0 ml/min). The injector temperature was set to ca. 250 °C, and a split injection mode was applied as required. The oven temperature programme was set as constant at ca. 40 °C. The FID signal sampling rate was ca. 50 s^{-1}.

Results and discussion

The properties of the meMFC

The particle size distribution and morphology of the meMFC were studied with a fibre image analyser and SEM. The fibre image analyses showed that the meMFC had a broad particle size distribution (Fig. 2). The material was principally disintegrated at the microscale, which is observable in the no. of fibre fines in the sample. The microscale (< 200 µm) contained up to 98% of the material. The material also contained up to 5% of a water-soluble fraction (molecular weight < 3.5 kDa), which comprises water-soluble sugars (enzymatic hydrolysis products (glucose and cellobiose) and water-soluble short polymers e.g. oligosaccharides (incompletely hydrolysed short cellulose cellulose and hemicellulose polymers).(Pere et al. 2020) In the SEM images, the microscale fibre fragments and nanoscale CNFs were visible (Fig. 4a and b). The largest fibre fragments had a diameter of several micrometres. The disintegrated material exhibited a visual appearance typical to coarse mechanically disintegrated microfibrillated cellulose (Nakagaito et al. 2004). The water-soluble polymers and sugars were not visible in the SEM images due to the resolution limits of the techniques.

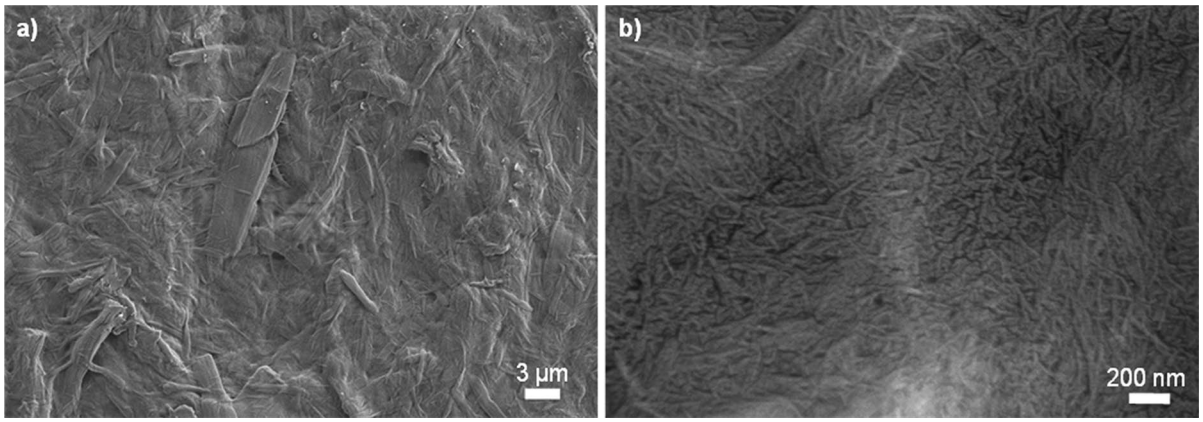

Fig. 4 The SEM images of the used meMFC show the polydispersity of the micro- (**a**) and nanoscale (**b**) fractions

These results are similar to the original study with the meMFC by Pere et al. (Pere et al. 2020).

The meMFC coating of the BVs

The meMFC was coated on the wet BV specimens using a spray-coating technique. The meMFC coating made the surface of the BVs look whiter (Fig. 5a). The used meMFC contain only a small amount of lignin, i.e., the brownish component in wood (Zhang et al. 2020). To the naked eye, the meMFC-coated specimens looked more natural than the uncoated specimens. The coated specimens were imaged with the SEM. The native BV surface was very rough, exhibiting open lumens and pores with sizes ranging from tens to hundreds of micrometres (Fig. 5b). The reason for the high SR of the BV surface was the rotary cutting method used. This method peeled the wood cell wall so that some of the fibres were cut in the grain direction, revealing fibre lumens (Bekhta et al. 2014). The meMFC coating significantly smoothened the BV surface, as seen in the SEM image (Fig. 5c). The surface morphology of the meMFC observed earlier (Fig. 4) was replicated on the BV surface (Fig. 5c). It is conceivable that the coating mechanism allowed the fibre fragments to fill the large pores while the microsized meMFC smoothened the surface, and the water-soluble fraction penetrated the surface pores.

The effect of the applied meMFC coating amount on the roughness (SR) of the BVs was measured using an optical profilometer. The root mean squared SR of the native BVs was ca. 4.7 ± 0.8 µm and decreased to ca. 3.7 ± 0.7 µm when one CL of the meMFC was applied to the BVs (Fig. 5d). The SR decreased linearly as a function of the applied CLs, and the smallest SR of ca. 1.8 ± 0.5 µm was observed with three CLs. The coat weight of one meMFC CL was ca. 29.0 ± 0.6 g/m^2, and the process parameters can be set in the spray-coating technology (Luangkularb et al. 2014). The multiple CLs increased the coat weight on the surface linearly. The highest coat weight was ca. 96.5 ± 4.8 g/m^2 with the three applied CLs. The sample standard deviation of the coat weightwas slight and shows that the spray-coating technique has a reasonable weight control for preparing thin CLs.

The compatibility, adhesion, and strength development of the meMFC-coated BVs

The FTIR technique was used to characterize the BV before and after coating with meMFC (Fig. 6a). Both samples exhibited all of the main peaks characteristic of lignocellulosic materials.(Emmanuel et al. 2015; Fan et al. 2012) Pure cellulose exhibits a typical cellulose fingerprint region (800–1200 cm^{-1}). The peak at 1150 cm^{-1} is resulted from asymmetric stretching (C–O–C). The peak at around 1000 cm^{-1} is resulted from C–C, C–OH, C–H bonds in a glucose ring and side group vibrations. The broad band in the 3600–3100 cm^{-1} range is due to the OH-stretching vibration of the hydroxyl groups on cellulose, hemicellulose, and lignin backbones, although bound water also contributes to this region. Lignin peaks are assaigned in the 1800−1500 cm^{-1} range.(Emmanuel et al. 2015) The peak at 1514 cm^{-1} is resulted from the aromatic C=C formation and the peak at

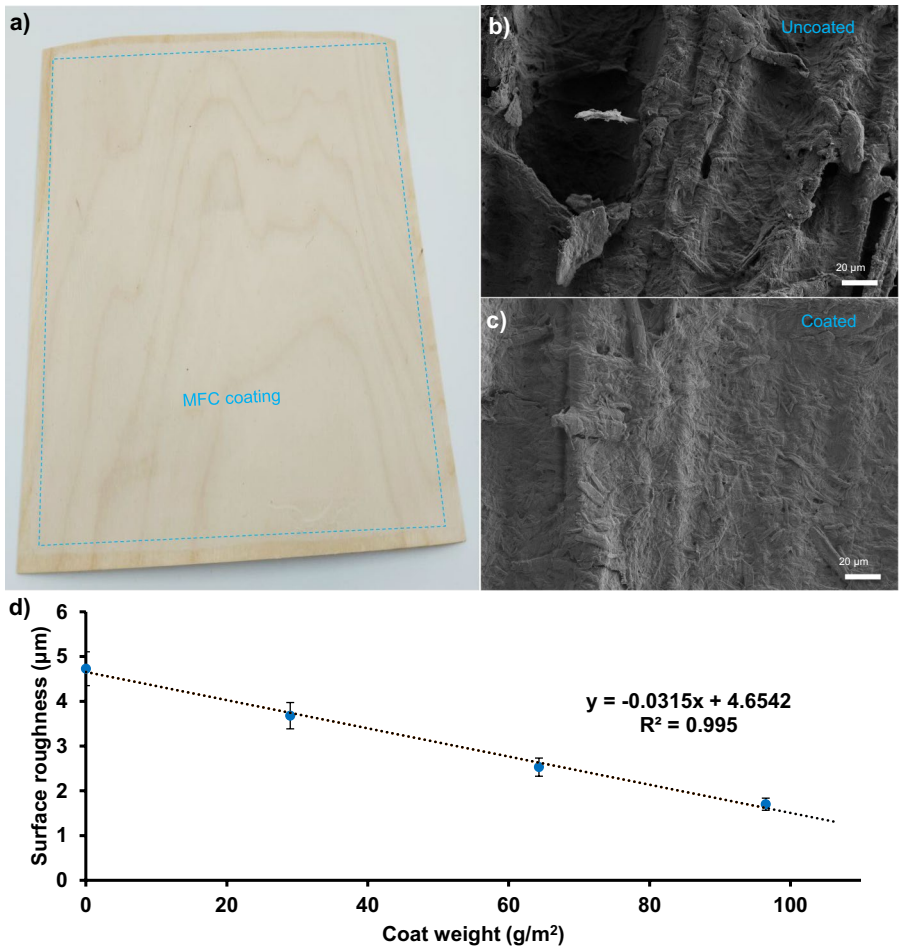

Fig. 5 **a** A photograph of a BV specimen with a meMFC coating. The dashed line has been placed in the image to show the borders of the coated area. The SEM images of the surface of the BV **b** before and **c** after applying one CL (29 g/m^2) of the meMFC. **d** The negative linear correlation between the coat weight (area density) and SR of the applied meMFC CLs

1720 cm^{-1} is the resulted from C=O stretching of the lignin. The FTIR results reveal that the signal from lignin is comprehensively blocked when the meMFC coating is applied on BV. The meMFC coating contains only a small fraction of lignin (see above) that is only weakly visible.

The compatibility of the meMFC and BVs was estimated using the WCA and SFE measurements. The WCA of the BVs and meMFC were 50° ± 2° (5 s) and below 10° ± 5° (5 s), respectively (Fig. 6b). The reason for this WCA difference is the lignin on the wood surface, which is not present in the meMFC (Pere et al. 2020). Lignin is the less hydrophilic component in LC. Pure mill wood lignin has a reported WCA of ca. 55° (Notley et al. 2010), and native cellulose has a reported WCA of ca. 25° (Mohan et al. 2011). These WCAs indicate that the native BV surface was chemically akin to the lignin surface, and the meMFC coating resembled pure cellulose. Earlier, for enzymatically-manufactured softwood NC, a WCA of ca. 18° was presented (Pere et al. 2020), which correlates with our results. The WCA value decreased slowly in the native BV specimens as the water droplets penetrated the wood pores. As similarly observed with the meMFC, this also indicates that the meMFC specimen was smoother and lacked suitable pores, so the effect was that the water could not evaporate rapidly. After 30 s, the WCA of the native BVs was ca. 30° ± 3°. The pre-treatment of the BV surfaces with sanding reduced the measured WCA to ca. 25° ± 2° (5 s) and 12° ± 2° (30 s). On wood materials, this can be explained by the accumulation of extractives on the wood surface that increases the WCAs (Hse et al. 1988). A similar effect is observed with thermomechanical pulp, where the behaviour is called "self-sizing", which explains why the hydrophobicity of mechanical pulp increases as the pulp ages (Bialczak et al. 2011).

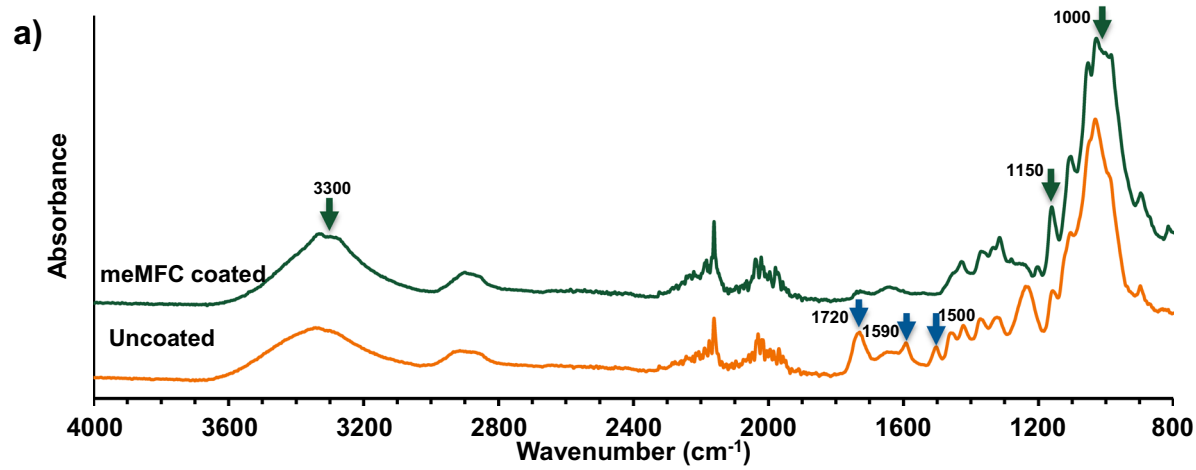

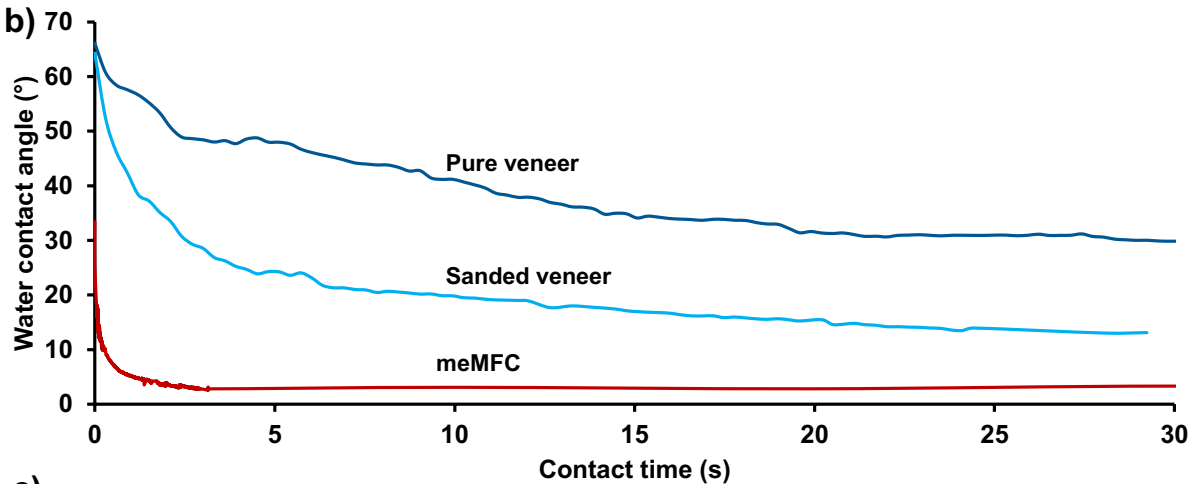

c)

Sample	Method	γtot [mN/m]	γd [mN/m]	γp [mN/m]	γ+	γ-
meMFC coating	Acid-Base	49.87	40.39	9.48	0.60	7.92
Pure veneer	Acid-Base	53.97	49.59	4.39	0.35	6.31

Fig. 6 **a** FTIR spectra of native BV before and after meMFC coating (coat weight 29 g/m^2). **b** The typical WCAs and **c** SFE components of the native BVs and meMFC. In addition, the WCAs of the sanded BV surfaces without the meMFC coating are also shown **b**

The first requirement for good adhesion between an adhesive and a substrate is that the adhesive evenly wets the substrate (Kinloch 1987). In surface tension terms, this means that the SFE of the substrate needs to be higher than that of the adhesive material. In water-based coating systems, the bond formation occurs when the water is evaporated from the spread CL, followed by the capillary force based action that pulls the coated material into contact with the surface of the substrate. The SFE of the meMFC was slightly smaller than that of the native BVs ($\gamma_{tot,meMFC} \approx 50$ mN/m vs. $\gamma_{tot,veneer} \approx 54$ mN/m) (Fig. 6c). The native BVs had a somewhat higher dispersive component and smaller polar component compared to the results of the meMFC. The reason for these observations was the presence of the more hydrophobic lignin and extractive components on the surfaces of the native BVs that do not exist on the meMFC. The slight differences between the SFEs indicate that the SFE matching between the meMFC and native BVs was not perfect, suggesting the use of pre-treatment techniques.

The adhesion of the meMFC onto the BVs and the mechanical strength of the coated BVs

The adhesion of the coated meMFC CLs on the BVs was measured using the pull-off measurements from the specimens coated on either dry or wet BVs (Fig. 7a). The pull-off forces of the meMFC CLs (both coated on dry and wet BVs) were 10 ± 4 N (0.10 MPa). The pre-treatment with the sanding increased the pull-off force of the meMFC coating to ca. 14 ± 4 N (0.15 MPa, coated on wet BVs) and ca. 24 N ± 5 (0.25 MPa, coated on dry BVs), respectively. The sanding is reported to influence the SR and chemical structure of the wood surfaces, enhancing coating adhesion (Sinn et al. 2004; Söğütlü et al. 2016; Thoma et al. 2015). As a reference, we tested if a commercial biodegradable water-based dispersion (BASF Epotal ECO 3675X) primer could further enhance the adhesion of the meMFC on the BVs. The adhesion of the meMFC on the BVs was increased to above ca. 40 ± 5 N (0.44 MPa), which indicates that the adhesion was doubled compared to the value measured on the sanded BV surfaces. The adhesion strengths were calculated above to correlate with the literature values. The adhesion values were smaller compared to the results obtained with commercial waterborne acrylic paints (adhesion strength up to ca. 5.0 MPa) and polyurethane coatings (up to ca. 1.0 MPa) (Turkulin et al. 2002). The most conceivable reason for the lower adhesion strengths is that the meMFC coating could not penetrate the pores of the wood surface to form the mechanical interlocks that polymeric paints can form.

The effects of the coating amount, BV thickness and drying methods were also investigated via a TTS test performed on the BV specimens coated with the meMFC (Fig. 7b and c). The results showed that all the coated BV specimens, except those with a 1.5 mm thickness, had higher TTSs than the reference, indicating that the coating with the meMFC could increase the TTSs of the BV specimens. The coated BV specimens that had been dried using a blower dryer (BD) tended to have better TTSs than those dried in a SC. It is possible that the active drying (BD) of the CLs promoted the attachment of the meMFC onto the BV wood surfaces, resulting in

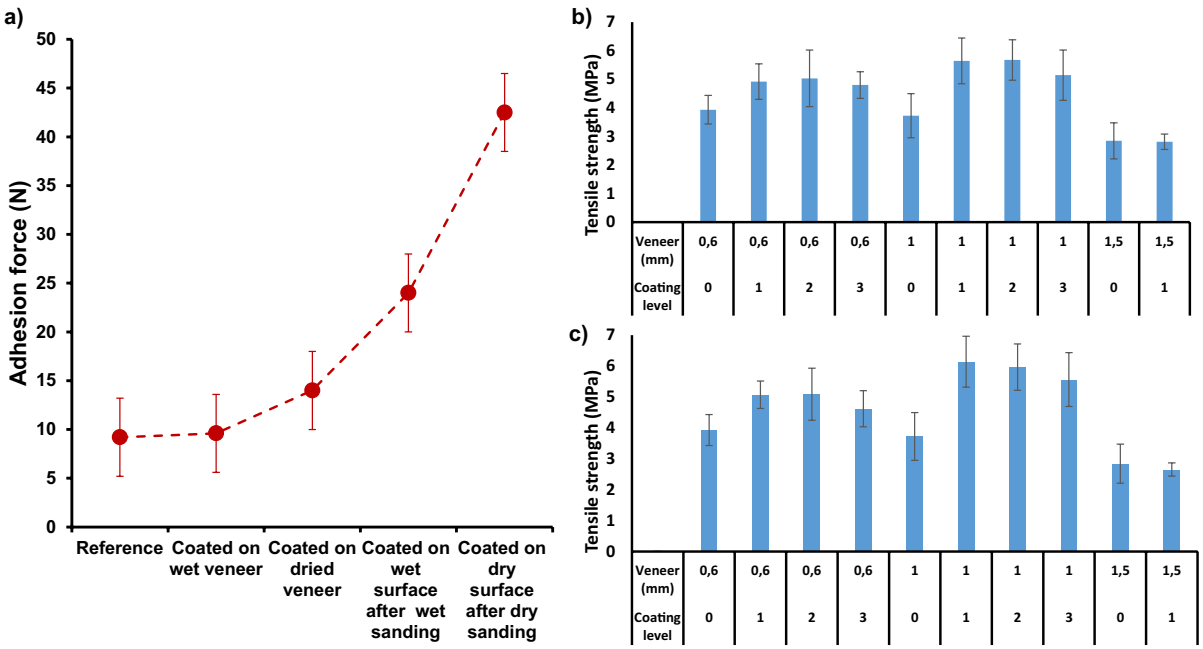

Fig. 7 **a** The adhesion force of the meMFC coating onto the BVs. The effects of the coating on the wet and dry surfaces and sanding are shown. The effect of a biodegradable primer is also shown. **b–c** The TTS of the meMFC-coated BV specimens with the three different coating levels and BV thicknesses, respectively. The coating levels were (1) 29.0 g/m^2, (2) 64.3 g/m^2, and (3) 96.5 g/m^2. The coated BV specimens were dried in: **b** a SC in the conditioning room or by **c** BD, which was conducted with an artificial hot-air dryer

higher TTSs. Although specific apparent differences were observed from the results of the BV specimens in 0.6 and 1.0 mm thickness, no significant differences were observed from the ones in 1.5 mm. The thick BV specimen was probably less flexible than the others, resulting in less elasticity and a higher likelihood of a weak point in the same specimen area, easily breakable during the test. The coating amount also affected the mechanical property performance in the BV specimens. The results indicated that the double-coated BV specimens tended to have lower TTSs than the other coated specimens. This finding suggests that excessive coating on the BVs reduces the adhesion between the meMFC and the wood surfaces.

Thermoresponsive meMFC coating with TC pigments

The meMFC was a binder for the two TC pigments to prepare a thermoresponsive (temperature-responsive) wood surface. The meMFC binds spherical TC pigments well and attaches them to the wood surface, as seen in the SEM image (Fig. 8a). The ability of NC materials to tightly bind various particles has also been reported earlier (Mattos et al. 2020). The TC pigments change their colour reversibly as the temperature rises above the transition temperature (Fig. 8b). In this study, the pigments used were black and orange with a transition temperature of ca. 28 °C. The pigment-doping influenced the deepness of the coating. It was observed that the specimen prepared with the ca. 8.0 wt.% consistency produced a deep colour. The colour disappeared quickly when the specimen was placed under a heat source. The colour change of the black pigments was more remarkable than the orange ones. It was observed that after 10 s of heating, the black pigment-doped specimen with a pigment loading below 8.0 wt.% reached the initial colour of the pure meMFC (Fig. 8c and d). The 20.0 wt.% black pigment loading did not produce as strong a colour transition, and some black pigment was visible after the heating. The probable reason was that the heat blower was not strong enough to heat the specimen thoroughly to activate all the TC pigments.

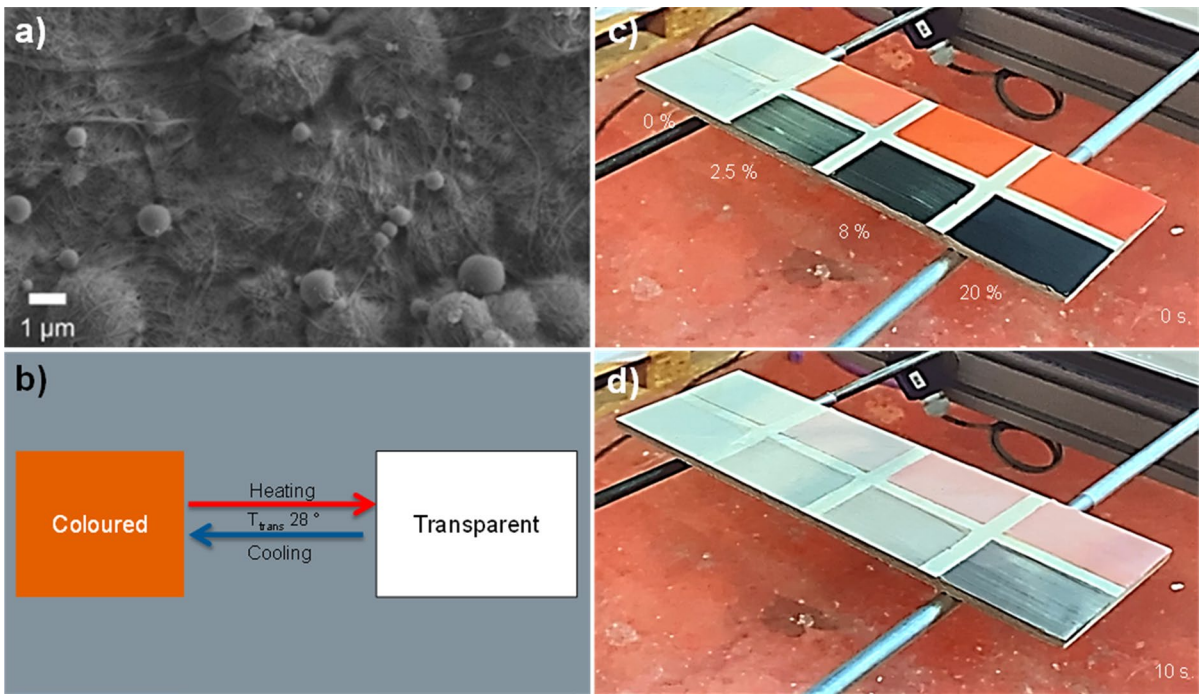

Fig. 8 **a** A SEM image of the TC pigment-doped meMFC coatings on the BVs. **b** The colour transition as the specimen surface temperature is switched. **c–d** The BV specimens with coated areas of two different colours (orange and black) of the meMFC TC coatings (the tested pigment consistencies were 0, ca. 2.5, ca. 8.0, and ca. 20.0 wt.%) **c** before and **d** after 10 s of warming under the hot-air blower

This lack of heating capability was also visible with the orange TC pigment-doped specimen, where the orange colour was more evident after the heating trial. A cycling test was performed by switching the heater on and off frequently.

The TC meMFC coating changed in colour over tens of heating cycles, and no irreversible changes were observed in the specimens. The maximum surface temperatures of the TC specimens in the laboratory test were monitored with a thermal camera (Fig. 9a). The black TC pigment specimens warmed more than the specimens made with the orange TC pigment. Overall, the shapes of all the warming curves were similar. The black specimens reached a surface temperature above 55 °C, whereas the orange specimens were ca. 10 °C lower in surface temperature. Studies on TC pigments in the wood coating field have been reported earlier. Li et al. (Li et al. 2017) used 2′-chloro-6′-(diethylamino) pigments to produce a colour-changing wood coating that displayed a reversible action when the temperature was cycled.

The warming of the TC meMFC coatings under the sun was tested in outdoor field tests. The functionality of the black TC pigment meMFC coating was compared to the black paint and a pure meMFC coating. Figure 9b presents the surface temperatures of all specimens as a function of the exposure time. The black surface warmed more quickly than the black TC meMFC surface, which can be seen in the higher slope value at ca. 0–1 min. All the specimens reached the first plateau during the first 5 min, indicating that the coating had become warm. The TC pigment-containing specimens changed their colour from black to white after a 1 min exposure. After 5 min, all measured surface temperatures continued to rise, and after 15 min, all specimens reached their final plateau levels. The black reference surface warmed to ca. 45 °C, whereas the surface temperature of the pure meMFC was ca. 10 °C lower.

The black TC pigment specimens followed a warming curve similar to the pure meMFC coating. Furthermore, there was no significant effect concerning the amount of TC pigment in the meMFC. These

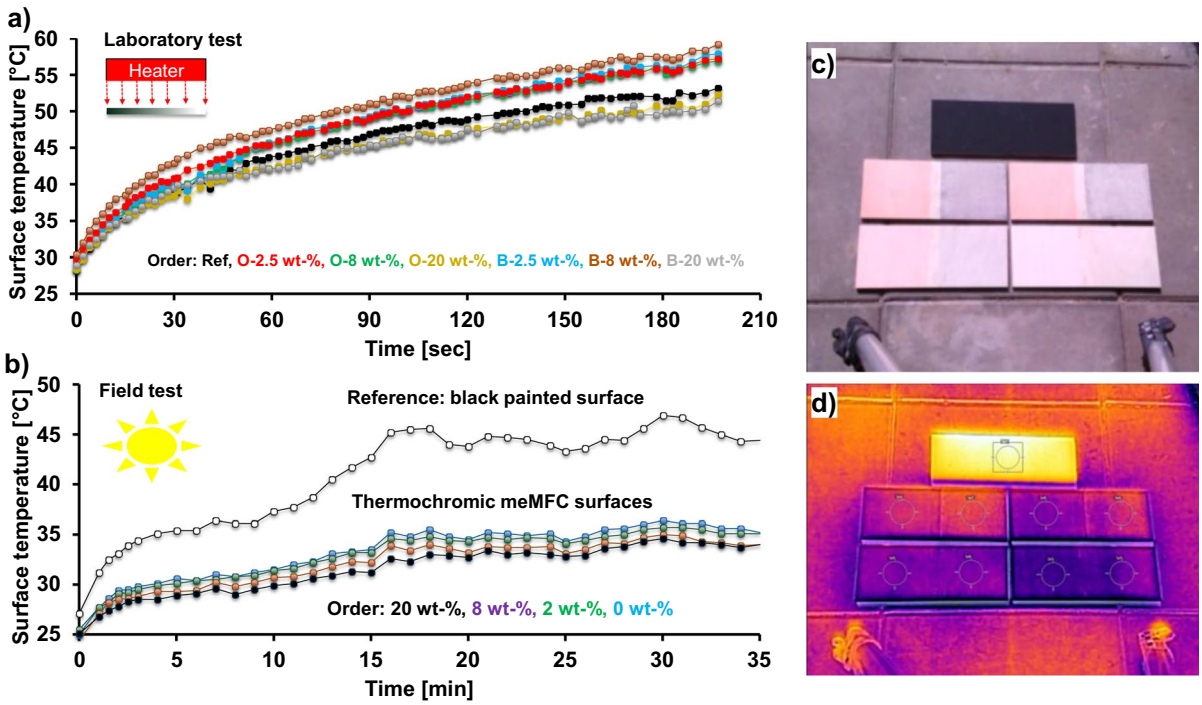

Fig. 9 **a** The surface temperatures of the TC meMFC-coated BV specimens under the heat blower as a function of the heating time. The specimen coding: O = the orange pigment, B = the black pigment, and the wt.%s identify the amount of the pigment in the meMFC. **b** The surface temperatures of the black TC meMFC-coated BVs in field testing. **c** A photography and **d** a heat camera image of TC specimens under sun light

results indicate that the black TC meMFC coating limits the warming of the wood surface under solar radiation when the temperature of the wood plate rises over 30 °C. In the literature, Zheng et al. (Zheng et al. 2015) reported that a TC coating worked best when the outside temperature rose over 25 °C during the year. The approach used in this study offers a simple method to attach functionalities to the BV surfaces.

The optical properties and PC activity of the meMFC coating doped with theTiO_2

The BV specimens were treated in a weathering device for 48 h, and the colour coordinates of each specimen were recorded over the period (Fig. 10). It is commonly known that a chromophore is formed on the surface of the wood when exposed to UV radiation. All the BV specimens turned darker during the weathering. A clear trend of the remaining lightness on the specimens coated with the TiO_2 exists.

Moreover, the degree of the effect seems to correlate with the concentration of the TiO_2 in the meMFC. Surprisingly, the UV-light-reflected effect was indicated in the specimen coated with only the meMFC. Hypothetically, the meMFC can be used solely for wood surfaces as a coating agent to prevent wood surface discolouration. A comparison of the colour differences (ΔE_{ab}) values in the specimens showed that the meMFC coatings markedly stabilised the wood surface colour during the weathering. The ΔE_{ab} refers to the degree of the colour changes over time compared to the measurement at zero. These findings suggest that the meMFC with the TiO_2 effectively prevents wood discolouration and stabilises the wood surface colour vs. UV radiation. As a further observation, the pure meMFC provides some of these effects without the TiO_2 doping.

A UV and fluorescent light tested the PC activity of the TiO_2 + meMFC vs. the air chemicals. The degree of the PC functionality was measured via the HCHO gas concentration reduction rate in the glass vials. The HCHO is a well-known VOC, a common indoor-air pollutant released from wood products like plywood (Uchiyama et al. 2007). Figure 10c and d show the summary of the photoactivation tests. Under both light sources, the concentrations of the HCHO have reduced in the TiO_2 + meMFC BV vials, and the

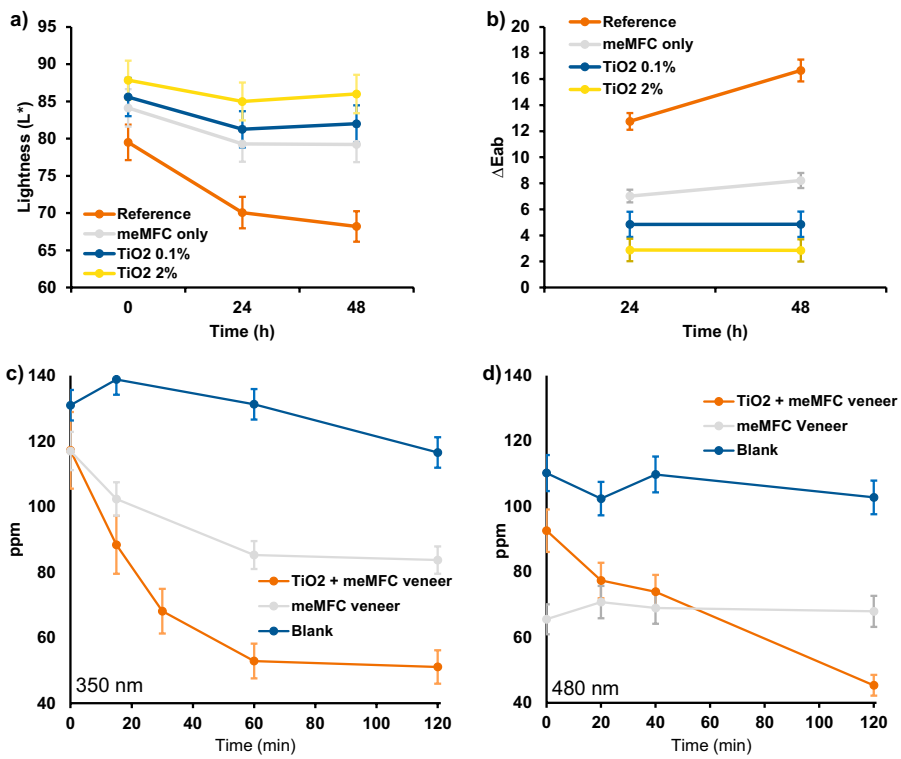

Fig. 10 The changes to the colour coordinates in the BV specimens during the weathering test: **a** The L^* scale (lightness) and **b** the ΔE_{ab} (the colour differences). For the ΔE_{ab} calculation, the colour coordinates at 0 h were used as references. The PC effects of the TiO_2 in the meMFC coating on the BV specimens under different light sources (**c**) and (**d**)

reduction rate was higher in the vial under UV light. The HCHO concentrations in the meMFC BV vial and the blank were also reduced under UV light. This reduction could probably be due to the photodegradation of the HCHO by the UV light itself (Shie et al. 2008). In all the vials, the initial gas concentrations varied. This variance could originate from differences in the gas dispersion rates, or some of the gas might have been absorbed or trapped in the wood pores at 0 h. Under the fluorescent light, no significant reduction in the concentration was observed in the blank and meMFC BVs, unlike the ones under UV light. Similar approach has earlier utilized to prepare an active surface that can remove indoor pollutans as formaldehyde (Ichiura et al. 2003).

Conclusions

The meMFC was used to coat the BVs, and it was spread on a BV surface using a spray-coating device. The spray coating controls the coat weight and makes it possible to coat thin CLs. The properties of the meMFC coating deposited on the BV surfaces were studied. The meMFC smoothens the BV surfaces and makes them whiter. The compatibility of the BVs and meMFC CLs was also studied. The adhesion of the meMFC on the BVs was investigated using SFE measurements. In their chemical profiles, the meMFC and BVs are similar, but the lignin and extractives on the surfaces of the BVs slightly decreased their hydrophilicity character. The adhesion of the meMFC to the BVs was investigated using pull-off measurements. Limited compatibility on the native BVs was seen in the low pull-off force, but this significantly improved when the BVs were pre-sanded or primer-coated. The good binding properties of NC were utilised to immobilise the TC pigments to the BV surfaces. The TC meMFC coating made the BVs temperature-responsive. The BV surfaces changed in colour when the BVs were heated with a hot-air blower. The warming of the TC meMFC-coated specimens in sunlight was measured using a heat camera. It was shown that the TC meMFC coating could be used to control the warming of the BVs under sunlight. The addition of the TiO_2 particles made the BV surfaces photoactive. The meMFC itself protected the wood surfaces against UV radiation. The added TiO_2 enabled the photoactivity that degraded the HCHO under UV light. The meMFC coating is a versatile binder to protect the wood and install functionalities to the wood surfaces.

Acknowledgments The authors would like to thank Panu Lahtinen for preparing the meMFC, Jaakko Pere for developing the project idea, and Vuokko Liukkonen for carrying out the contact angle and optical profilometer measurements. This work was a part of the Flagship Programme of the Academy of Finland under Project Nos. 318890 and 318891 (Competence Center for the Materials Bioeconomy, FinnCERES).

Author contributions All authors contributed to the study conception and design.The manuscript was written through contributions from all authors. HO was responsible for preparing the project plan, instructing the research work and writing the first draft of the article. VK was responsible for preparing the meMFC and carrying out coating trials. AY was responsible for the tensile measurements of the coated BVs. MV continued the work of AY and proofread and reviewed this manuscript. LR developed the measurement plan and steered the work. Finally, AK was responsible for steering the research. The manuscript was written with contributions from all the authors. All the authors have approved the final version of the manuscript.

Funding Open Access funding provided by Technical Research Centre of Finland (VTT). This study was carried out in the Verycoat (Novel high-performance veneer products by effective drying and nano-coating) project funded by Business Finland and supported by Finnish industrial companies (Stora-Enso Oyj., Raute Ltd., Koskisen Oy, Teknos Oy, Puustelli Oy, A-Factory Oy).

Data availability The corresponding author will provide the datasets generated for this study on request. The data is stored in the VTT's server.

Declarations

Competing interests The authors have no relevant financial or non-financial interests to disclose.

Ethics approval Not applicable. This article does not contain any studies with human participants or anamials performed by any of the authors.

References

Abdellaoui H, Raji M, Chakchak H, Bouhfid R (2020) Thermochromic composite materials: synthesis, properties and applications. Rachid Bouhfid AeKQ, Mohammad Jawaid (ed) polymer nanocomposite-based smart materials. Woodhead Publishing, Elsevier

Ahonen T (1995) Remontti: Maalaus-ja korjaustyöt. RAK Rakennusalan kustantajat, Finland

Bekhta P, Proszyk S, Krystofiak T, Mamonova M, Pinkowski G, Lis B (2014) Effect of thermomechanical densification on surface roughness of wood veneers. Wood Mat Sci Eng 9:233–245. https://doi.org/10.1080/17480272.2014.923042

Bergman R, Puettmann M, Taylor A, Skog KE (2014) The carbon impacts of wood products. For Prod J 64:220–231. https://doi.org/10.13073/fpj-d-14-00047

Bialczak S, Holmbom B, Sundberg A, Peltonen J (2011) Mechanical pulping: changes in extractives and wetting properties of TMP paper during ageing. Nordic Pulp Pap Res J 26:438–444. https://doi.org/10.3183/npprj-2011-26-04-p438-444

Bulian F, Graystone J (2009) Wood coatings: theory and practice. Elsevier, Amsterdam

Chen F, Yang X, Wu Q (2009) Antifungal capability of TiO2 coated film on moist wood. Build Environ 44:1088–1093. https://doi.org/10.1016/j.buildenv.2008.07.018

Cheng D, Wen Y, An X, Zhu X, Ni Y (2016) TEMPO-oxidized cellulose nanofibers (TOCNs) as a green reinforcement for waterborne polyurethane coating (WPU) on wood. Carbohydr Polym 151:326–334. https://doi.org/10.1016/j.carbpol.2016.05.083

Croll SG, Kleinlein RL (1986) Water-Soluble polymers. American Chemical Society

Emmanuel V, Odile B, Céline R (2015) FTIR spectroscopy of woods: a new approach to study the weathering of the carving face of a sculpture. Spectrochim Acta Part A 136:1255–1259. https://doi.org/10.1016/j.saa.2014.10.011

Ennos R (2020) The age of Wood: our most useful material and the construction of civilization. Scribner

Fan M, Dai D, Huang B (2012) Fourier transform infrared spectroscopy for natural fibres. In: Salih SM (ed) Fourier transform-materials analysis, IntechOpen, pp 45–68

Fujishima A, Honda K (1972) Electrochemical photolysis of water at a semiconductor electrode. Nature 238(5358):37–38. https://doi.org/10.1038/238037a0

Higuchi T (1985) Biosynthesis and biodegradation of wood components. Elsevier Science, Academic Press

Hse C-Y, Kuo M-l (1988) Influence of extractives on wood gluing and finishing-a review. For Prod J 38:52–56

Hubbe MA, Ferrer A, Tyagi P, Yin Y, Salas C, Pal L, Rojas OJ (2017) Nanocellulose in thin films, coatings, and plies for packaging applications: a review. Bioresour 12:2143–2233. https://doi.org/10.15376/biores.12.1.2143-2233

Ichiura H, Kitaoka T, Tanaka H (2003) Removal of indoor pollutants under UV irradiation by a composite TiO_2–zeolite sheet prepared using a papermaking technique. Chemosphere 50:79–83. https://doi.org/10.1016/S0045-6535(02)00604-5

Karlessi T, Santamouris M, Apostolakis K, Synnefa A, Livada I (2009) Development and testing of thermochromic coatings for buildings and urban structures. Sol Energy 83:538–551. https://doi.org/10.1016/j.solener.2008.10.005

Kinloch AJ (1987) Adhesion and adhesives: science and technology. Springer, New York

Klar V, Pere J, Turpeinen T, Kärki P, Orelma H, Kuosmanen P (2019) Shape fidelity and structure of 3D printed high consistency nanocellulose. Sci Rep 9:3822. https://doi.org/10.1038/s41598-019-40469-x

Klemm D, Philipp B, Heinze T (1998) Comprehensive cellulose chemistry, vol 2. Functionalization of cellulose. VCH, Weinheim

Kocaefe D, Huang X, Kocaefe Y (2015) Dimensional stabilization of Wood. Curr For Rep 1:151–161. https://doi.org/10.1007/s40725-015-0017-5

Lavoine N, Desloges I, Dufresne A, Bras J (2012) Microfibrillated cellulose - its barrier properties and applications in cellulosic materials: a review. Carbohydr Polym 90:735–764. https://doi.org/10.1016/j.carbpol.2012.05.026

Li Y, Hui B, Li G, Li J (2017) Fabrication of smart wood with reversible thermoresponsive performance. J Mater Sci 52:7688–7697. https://doi.org/10.1007/s10853-017-1036-3

Liu H, Liu Z, Liu H, Hui L, Zhang F, Liu P, An X, Wen Y, Wu S (2019) Using cationic nanofibrillated cellulose to increase the precipitated calcium carbonate retention and physical properties during reconstituted tobacco sheet preparation. Ind Crops Prod 130:592–597. https://doi.org/10.1016/j.indcrop.2019.01.021

Luangkularb S, Prombanpong S, Tangwarodomnukun V (2014) Material consumption and dry film thickness in spray coating process. Procedia CIRP 17:789–794. https://doi.org/10.1016/j.procir.2014.02.046

Mattos BD, Tardy BL, Greca LG, Kämäräinen T, Xiang W, Cusola O, Magalhães W, Rojas O (2020) Nanofibrillar networks enable universal assembly of superstructured particle constructs. Sci Adv 6:eaaz7328. https://doi.org/

Mohan T, Kargl R, Doliška A, Vesel A, Köstler S, Ribitsch V, Stana-Kleinschek K (2011) Wettability and surface composition of partly and fully regenerated cellulose thin films from trimethylsilyl cellulose. J Colloid Interface Sci 358:604–610. https://doi.org/10.1016/j.jcis.2011.03.022

Moon R, Martini A, Nairn J, Simonsen J, Youngblood J (2011) Cellulose nanomaterials review: structure, properties and nanocomposites. Chem Soc Rev 40:3941–3994. https://doi.org/10.1039/C0CS00108B

Nakagaito AN, Yano H (2004) The effect of morphological changes from pulp fiber towards nano-scale fibrillated cellulose on the mechanical properties of high-strength plant fiber based composites. App Phys A 78(4):547–552. https://doi.org/10.1007/s00339-003-2453-5

Notley SM, Norgren M (2010) Surface energy and wettability of spin-coated thin films of lignin isolated from wood. Langmuir 26:5484–5490. https://doi.org/10.1021/la1003337

Österberg M, Vartiainen J, Lucenius J, Hippi U, Seppälä J, Serimaa R, Laine J (2013) A fast method to produce strong NFC Films as a platform for barrier and functional materials. ACS Appl Mater Interfaces 5:4640–4647. https://doi.org/10.1021/am401046x

Pandit SK, Tudu BK, Mishra IM, Kumar A (2020) Development of stain resistant, superhydrophobic and self-cleaning coating on wood surface. Prog Org Coat 139:105453. https://doi.org/10.1016/j.porgcoat.2019.105453

Pánek M, Šimůnková K, Novák D, Dvořák O, Schönfelder O, Šedivka P, Kobetičová K (2020) Caffeine and TiO_2 nanoparticles treatment of spruce and beech wood for increasing transparent coating resistance against UV-Radiation and Mould attacks. Coatings 10(12):1141. https://doi.org/10.3390/coatings10121141

Pere J, Tammelin T, Niemi P, Lille M, Virtanen T, Penttilä PA, Ahvenainen P, Grönqvist S (2020) Production of high solid nanocellulose by enzyme-aided Fibrillation coupled with mild mechanical treatment. ACS Sustainable Chem Eng 8:18853–18863. https://doi.org/10.1021/acssuschemeng.0c05202

Pori P, Vilčnik A, Petrič M, Sever Škapin A, Mihelčič M, Šurca Vuk A, Novak U, Orel B (2016) Structural studies of TiO_2/wood coatings prepared by hydrothermal deposition of rutile particles from TiCl4 aqueous solutions on spruce (Picea Abies) wood. Appl Surf Sci 372:125–138. https://doi.org/10.1016/j.apsusc.2016.03.065

Ramage MH, Burridge H, Busse-Wicher M, Fereday G, Reynolds T, Shah DU, Wu G, Yu L, Fleming P, Densley-Tingley D, Allwood J, Dupree P, Linden PF, Scherman O (2017) The wood from the trees: the use of timber in construction. Renew Sustain Energy Rev 68:333–359. https://doi.org/10.1016/j.rser.2016.09.107

Rao X, Liu Y, Fu Y, Liu Y, Yu H (2016) Formation and properties of polyelectrolytes/TiO_2 composite coating on wood surfaces through layer-by-layer assembly method. Holzforschung 70(4):361–367. https://doi.org/10.1515/hf-2015-0047

Saito T, Nishiyama Y, Putaux J-L, Vignon M, Isogai A (2006) Homogeneous suspensions of Individualized microfibrils from TEMPO-catalyzed oxidation of native cellulose. Biomacromolecules 7:1687–1691. https://doi.org/10.1021/bm060154s

Sathre R, Gustavsson L (2009) Using wood products to mitigate climate change: external costs and structural change. Appl Energy 86:251–257. https://doi.org/10.1016/j.apenergy.2008.04.007

Shie J-L, Lee C-H, Chiou C-S, Chang C-T, Chang C-C, Chang C-Y (2008) Photodegradation kinetics of formaldehyde using light sources of UVA, UVC and UVLED in the presence of composed silver titanium oxide photocatalyst. J Hazard Mater 155:164–172. https://doi.org/10.1016/j.jhazmat.2007.11.043

Sinn G, Gindl M, Reiterer A, Stanzl-Tschegg S (2004) Changes in the surface properties of wood due to sanding. 58:246–251. https://doi.org/10.1515/HF.2004.038

Siró I, Plackett D, Hedenqvist M, Ankerfors M, Lindström T (2011) Highly transparent films from carboxymethylated microfibrillated cellulose: the effect of multiple homogenization steps on key properties. J Appl Polym Sci 119:2652–2660. https://doi.org/10.1002/app.32831

Standardization CECf (2004) Plywood - Bonding quality - Part 1: Test methods. Brussels

Stoye D, Funke W, Hoppe L, Hasselkus J, Curtis LG, Hoehne K, Zech H-J, Heiling P, Yamabe M, Dören K, Schupp H, Küchenmeister R, Schmitthenner M, Kremer W, Wieczorrek W, Gempeler H, Schneider W, White JW, Short AG, Blank WJ, Calbo LJ, Plath D, Wagner F, Haller W, Rödder K-M, Streitberger H-J, Urbano E, Laible R, Meyer BD, Bagda E, Waite FA, Philips M, Köhler K, Simmendinger P, Roelle W, Scholz W, Kortmann W, Valet A, Slongo M, Molz T, Hiller R, Thomer KW, Vogel K, Schernau U, Hüser B, Brandt A, Milne A, Weyers H, Plehn W, Lentze H-A (2000) Paints and coatings, Ullmann's Encyclopedia of Industrial Chemistry, Wiley-VCH

Söğütlü C, Nzokou P, Koc I, Tutgun R, Döngel N (2016) The effects of surface roughness on varnish adhesion strength of wood materials. J Coat Technol Res 13:863–870. https://doi.org/10.1007/s11998-016-9805-5

Taha H, Sailor DJ, Akbari H (1992) High-albedo materials for reducing building cooling energy use. Lawrence Berkeley Lab. CA (United States)

Thoma H, Peri L, Lato E (2015) Evaluation of wood surface roughness depending on species characteristics. Maderas Ciencia y tecnología 17:285–292. https://doi.org/10.4067/S0718-221X2015005000027

Turkulin H, Richter K, Sell J (2002) Adhesion of water-borne acrylic and hybrid paint on wood treated with primers. Surf Coat Int: Part B 85:273–280. https://doi.org/10.1007/BF02699550

Uchiyama S, Matsushima E, Kitao N, Tokunaga H, Ando M, Otsubo Y (2007) Effect of natural compounds on reducing formaldehyde emission from plywood. Atmos Environ 41:8825–8830. https://doi.org/10.1016/j.atmosenv.2007.09.046

Uddin KMA, Orelma H, Mohammadi P, Borghei M, Laine J, Linder M, Rojas OJ (2017) Retention of lysozyme activity by physical immobilization in nanocellulose aerogels and antibacterial effects. Cellulose 24:2837–2848. https://doi.org/10.1007/s10570-017-1311-0

Xing D, Zhang Y, Hu J, Yao L (2020) Highly hydrophobic and self-cleaning heat-treated *Larix* spp. Prepared by TiO2 and ZnO particles onto wood surface. Coatings 10:986. https://doi.org/10.3390/coatings10100986

Yamamoto A, Rohumaa A, Hughes M, Vuorinen T, Rautkari L (2017) Surface modification of birch veneer by peroxide bleaching. Wood Sci Tech 51:85–95. https://doi.org/10.1007/s00226-016-0880-7

Yamamoto A, Rohumaa A, Kontturi E, Hughes M, Vuorinen T (2015) The effect of hydrothermal treatment on the color stability and chemical properties of birch veneer surfaces. Bioresources 10:6610–6623. https://doi.org/10.15376/biores.10.4.6610-6623

Yano H, Omura H, Honma Y, Okumura H, Sano H, Nakatsubo F (2018) Designing cellulose nanofiber surface for high density polyethylene reinforcement. Cellulose 25:3351–3362. https://doi.org/10.1007/s10570-018-1787-2

Yuan B, Guo M, Huang Z, Naik N, Hu Q, Guo Z (2021) A UV-shielding and hydrophobic graphitic carbon nitride nanosheets/cellulose nanofibril (gCNNS/CNF) transparent coating on wood surface for weathering resistance. Prog Org Coat 159:106440. https://doi.org/10.1016/j.porgcoat.2021.106440

Zhang H, Fu S, Chen Y (2020) Basic understanding of the color distinction of lignin and the proper selection of lignin in color-depended utilizations. Int J Biol Macromol 147:607–615. https://doi.org/10.1016/j.ijbiomac.2020.01.105

Zheng S, Xu Y, Shen Q, Yang H (2015) Preparation of thermochromic coatings and their energy saving analysis. Sol Energy 112:263–271. https://doi.org/10.1016/j.solener.2014.09.049

Zhu XD, Liu Y, Shen J (2016) Volatile organic compounds (VOCs) emissions of wood-based panels coated with nanoparticles modified water based varnish. Eur J Wood Wood Prod 74:601–607. https://doi.org/10.1007/s00107-016-1012-7